Physics and Chemistry of the Earth xxx (xxxx) xxx–xxx

Contents lists available at ScienceDirect

Physics and Chemistry of the Earth

journal homepage: www.elsevier.com/locate/pce

Study on microclimate observation network for urban unit: A case study in a campus of Shenzhen, China

Xin Lai[a], Yang Tang[b], Lei Li[a,*], PakWai Chan[c], Qingfeng Zeng[a]

[a] Shenzhen National Climate Observatory, Shenzhen, Guangdong, 518040, China
[b] Shenzhen Bixuange Company, Shenzhen, Guangdong, 518131, China
[c] Hong Kong Observatory, Kowloon, Hong Kong, 999077, China

ARTICLE INFO

Keywords:
Urban unit
Microclimate
Indoor climate
Observation

ABSTRACT

Urban units are city components that have relatively pure functions while carry a large number of urban residents. The quality of an urban unit's microclimate environment is closely related to the health and comfort of its population. In this study, we develop a technology on microclimate observation for urban units, which is experimentally applied in a campus in Shenzhen, China. We have arrived at the following conclusions: (1) The application of precision integration technology and small sensors greatly reduces the physical size of the microclimate observation instrument. With the help of advanced algorithms for data quality control, the cost of detection and measuring instruments can be greatly reduced even when accuracy is maintained so that the instruments can be densely deployed in urban units. (2) The urban unit microclimate observation network, as a supplement to the traditional meteorological observation system, makes up for the deficiencies of coarse resolution and limited capability of the traditional observation system on describing urban heterogeneity, and can be used to more precisely depict the heterogeneity of the microclimate within the urban units. Utilizing the technology of Internet of things, it provides data support for people, who work, live and study in the urban units, to take appropriate measures to regulate microclimate environment, and also provides external parameters for automatic adjustment and control of smart air conditioners and dehumidifiers. (3) Temperature monitoring data show that the detected daily temperature ranges of the indoor stations within urban unit are relatively small, and the daily average temperatures observed by the indoor stations are quite different from those observed by the automatic weather stations located in open spaces, indicating that conventional meteorological observation has little reference value to the indoor environment of urban units. At the same time, the observed data of the different indoor monitoring points are quite different from each other, which are closely related to their specific environments. (4) Analysis of relative humidity data shows that the rules of variation of indoor relative humidity are quite different from those of open space, and indoor crowd and monitoring point environment may affect the indoor relative humidity.

1. Introduction

Since the industrial revolution, the speed of urbanization has accelerated all over the world, and more and more people are moving into cities. In order to carry more people, the area of a city keeps expanding, and the number of high-rise buildings increases gradually, greatly changing the physical properties of the city's underlying surface. And the change of the physical properties of the underlying surface of the city changes the original energy exchange process between the earth and the atmosphere, which has significant effects on the local climate in urban areas (Grimmond, 2007; Oke, 1997). This effect is superimposed on the effect of global warming and causes the drastic change of the local climate (McCarthy et al., 2010). Generally, the increase in the air temperature caused by the urbanization is between 1 and 3 °C. However, under some steady weather conditions, the air temperature difference between urban and suburb areas can reach as high as 10 °C (Oke, 1981). In some cities, the urbanization may contribute up to more than 80% of the local warming, and has become the most determinative factor of the urban climatic environment (Li et al., 2015). In addition to an overall increase trend in air temperature, it has been observed in quite a number of cities a decrease trend of the diurnal temperature range, which is also caused by the urbanization and other changes of the land use (Kalnay and Cai, 2003). In subtropical or tropical regions, a reduction of the diurnal temperature range means that it is difficult for

* Corresponding author.
E-mail address: chonp@163.com (L. Li).

https://doi.org/10.1016/j.pce.2018.08.003
Received 12 June 2018; Received in revised form 12 August 2018; Accepted 16 August 2018

the daytime heat to dissipate at night in the summer, which means the deterioration of the climatic comfort in urban areas.

While the urbanization leads to local warming, urban residents' pursuit of the quality of climatic environment is constantly increasing along with the development of the material civilization. One of the most basic needs is the demand for the information on the quality of the climatic environment, that is, to understand the microclimate and environment in which he or she is located or plan to travel to, which will help to provide reference for taking measure to obtain a more comfortable and safer environment for travel, working and living. This is especially evident in countries that are rapidly developing, such as China. Shenzhen is the fastest urbanizing city in China. Over the last 40 years, it has developed from a small county with a population of only a few hundred thousand into one of the 4 most developed and affluent cities in China. At present, there are more than 10 million people living in Shenzhen (Li et al., 2015), of which quite a lot of them are well-educated new immigrants who have strong demands for information on the quality of the climatic environmental, including air temperature, humidity and pollutant concentration.

In order to provide Shenzhen citizens the information service on the quality of the climatic environment as well as meteorological disasters information services, the Meteorological Bureau of Shenzhen Municipality has deployed a large number of detection and measuring instruments in the city to detect and measure urban meteorological data in open space. More than 180 automatic weather stations have been built on less than 2000 square kilometers of land in Shenzhen. However, despite the fact that the number of the detection and measuring instruments is sufficiently large, the traditional meteorological observation can still not fully meet the increasingly sophisticated demand of the Shenzhen residents for the information on the quality of environment. This is mainly manifested in three aspects: (1) limited by high price and harsh installation environment, the number of automatic weather stations cannot be increased indefinitely; (2) the meteorological elements are highly heterogeneous within cities, and the limited number of stations have limited capability to be used to describe such heterogeneity; (3) the Shenzhen residents spend quite a lot of time working and living indoors, and the data provided by the detection and measuring instruments in the open space are not representative to the quality of indoor environment. Under this background, the urban microclimate services focused on the observation of the microclimate environment within urban units are put forward. As a necessary supplement to the traditional meteorological observations, the observations within urban units are no longer limited to be located in outdoor open spaces, and, unlike traditional meteorological observation, do not require a certain scale of regional representation (WMO, 2017). In general, the term “urban unit” can be defined as an urban component with relatively pure functions. It usually includes several buildings and supporting open space which provide the spaces for the urban residents to live, work, study, receive treatment or rest, such as schools, hospitals, parks, shopping malls and so on.

At present, there have been some studies focused on indoor microclimate and its control (Fountain et al., 1996; Morgan and de Dear, 2003; Silva et al., 2016; Hilliaho et al., 2016). However, little literature is found to be focused on comparative analysis on the microclimate of different indoor locations. In this study, a technology on microclimate observation for urban units is established. Based on the technology, observation instruments can be densely deployed in an urban unit according to the characteristics of the urban unit and the customized demand to comprehensively monitor the microclimate in the unit. The data collected by the urban unit microclimate observation network can provide basic data for supporting taking measures to optimize the environment and protect the people in the urban unit. These data can also lay a foundation for further studies on the characteristics, the variation rules and the mechanisms of the microclimate in urban units with different building envelopes and different functions, and thus have significant scientific values.

2. Working principle of equipment

2.1. Data acquisition and transmission process

There are actually many elements related to the microclimatic environment of urban units, including air temperature, humidity and ultraviolet radiation that are closely related to the human health and the comfort. Due to the fact that a considerable number of observation instruments in urban units need to be deployed in indoor environments, the measurement of wind is unnecessary and excluded. Using the precision integration technology, we integrate the sensors for measuring 6 other elements related to the human health into the observation instrument, namely, $PM_{2.5}$, formaldehyde, light, TVOC, noise and CO_2. All the sensors are produced by relevant professional manufacturers, which are carefully integrated to ensure one working sensor doesn't affect another working one. The sensors used are all miniaturized low cost sensors, which greatly reduce the physical size of the observation instrument. The size of the observation instrument developed in this study is only 30 cm * 6 cm * 8 cm, which can measure the 9 climatic and environmental elements mentioned above. The size of the observation instrument is far smaller than that of the automatic weather station's 40 cm * 40 cm * 1000 cm, and is even smaller than that of the temperature and humidity sensor of a professional automatic weather station.

The working principle of the whole equipment is shown in Fig. 1. The shape of the equipment is shown on the top of the left dotted line frame in Fig. 1. In the light of the normal height of human movement, the equipment is fixed on the wall at a height of around 2.2 m above the ground. There are totally 9 sensors integrated in the equipment, which transmits data to a local server via Multi Cluster Network Protocol (MCNP), and processes data on the server. On the local server, the data are controlled and processed to be able to more accurately reflect the quality of microclimate and environment of urban units. The processed

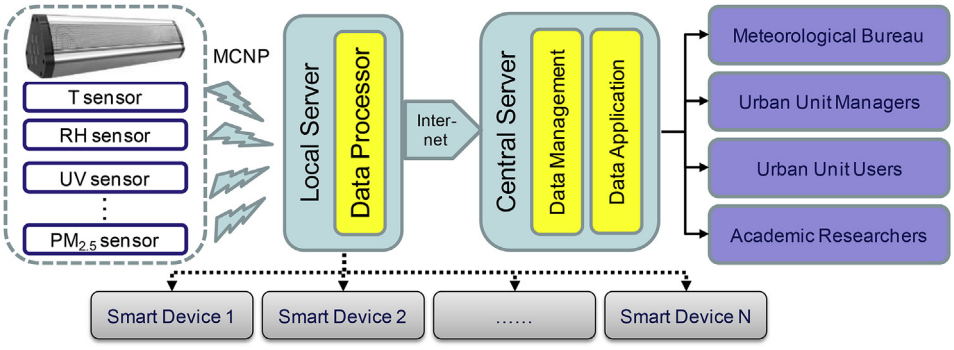

Fig. 1. The conception framework of the microclimate observation for the urban units.

data on the local server will go out in two directions, respectively: one path links the local server with some smart devices inside the urban unit, and is used to automatically control the microclimatic environment in the unit, for example, to adjust the air conditioning switch according to the air temperature, or to adjust the humidifier according to the humidity, etc.; the other path links the local server of the urban unit with the central server, which then distributes the data to the users, the data management organization (meteorological bureau) or the scientific researchers who need the data. The data transferred to the urban unit users can be further processed and rendered to generate graphics products to provide vivid and distinct information services for the users.

2.2. Quality control and processing of data

The accuracy of the data is a basic prerequisite for the data to be used in the next step service or study. The data processor on the local server consists of 3 modules, namely, the judgment module, training module and correction module. All collected data are sent to the central server only after being tested and revised by the data processor to ensure the accuracy of the observed data. The main functions of the three modules are as follows:

2.2.1. Judgment module

The main function of the judgment module is to test the authenticity of the observed data, which is the key to quality control of all observed meteorological data (Wolfson et al., 1978; Evans et al., 2003). The main methods used are the extreme value test, the temporal consistency test and the spatial consistency test. The test process is as follows:

(1) Obtain the observed value of a meteorological element at the current observation point and the present time x';
(2) Perform the measurement of the extreme values, which are preset and are generally the historical extremes of the meteorological element x' from the local meteorological observatory. The extreme value detection coefficient (α_1) of the observed value (x') of the current time is calculated by formula (1):

$$\alpha_1 = \mathrm{sgn}((x' - k_l)(k_u - x') + \lambda)\frac{|2x' - (k_u + k_l)|}{2(k_u - k_l)} \tag{1}$$

wherein sgn(·) stands for sign function, λ stands for positive infinitesimal, and $k_l \sim k_u$ stands for the observed interval extremum.

(3) Perform the temporal consistency detection on x' to obtain the temporal consistency detection coefficient α_2 of the observed value x' at the current time. Sequentially calculate the difference between the adjacent two observed data in the historically observed data X_H within T hours prior to the current time, $D_{X_H} = \{x_{j+1} - x_j | j = 1,2,...,T \times S - 1\}$, and the difference between the current observed value and the last observed value, $d_{x'} = x' - x_1$, wherein $T \times S$ historically observed data within T hours prior to the current time are represented by $X_H = \{x_i | i = 1,2,...,T \times S\} \in \mathbb{R}^{(T\times S)\times 1}$, wherein S stands for the number of times of sampling for the meteorological element per hour;

The temporal consistency detection coefficient of the observed data α_2 at the current time is calculated by using formula (2):

$$\alpha_2 = \mathrm{sgn}\big((d_{x'} - \tau_l)(\tau_u - d_{x'}) + \lambda\big)\frac{|2d_{x'} - (\tau_u + \tau_l)|}{2(\tau_u - \tau_l)} \tag{2}$$

wherein $\tau_l = \min(D_{X_H})$ stands for the lower boundary value of the range of the observed data within T hours prior to the current time, $\tau_u = \max(D_{X_H})$ stands for the upper boundary value of the range of the observed data within T hours prior to the current time.

(4) Spatial consistency detection is performed on x' to obtain the spatial consistency detection coefficient α_3 of the observed value x' at the current time. Remove the maximum and minimum values of the current data X_R of the C adjacent observation nodes to obtain the reference data for the $C - 2$ adjacent observation nodes, and obtain the fitting value of the current observation node via formula (3):

$$x = \sum_{k=1}^{C-2} \frac{x'_k}{p_k z_k^m} \Big/ \sum_{k=1}^{C-2} \frac{1}{p_k z_k^m} \tag{3}$$

wherein z_k stands for the spatial distance between the kth adjacent observation node and the current observation node, p_k stands for the relative measurement accuracy of the current sensor, m stands for the exponential term for controlling distance weight, the current observed values of the C observed nodes adjacent to the current observational node in spatial geographic location are represented by $X_R = \{x'_k | k = 1,2,...,C\} \in \mathbb{R}^{1\times C}$;

Based on the fitting values and the measured values of the observed nodes, calculate the spatial consistency detection coefficient α_3 by using formula (4).

$$\alpha_3 = \frac{|x - x'|}{\delta_u - \delta_l} \tag{4}$$

wherein $\delta_l = \min\{x'_k | k = 1,2,...,C-2\}$ stands for the lower boundary value of the reference data of the adjacent $C - 2$ observation nodes, and $\delta_u = \max\{x'_k | k = 1,2,...,C-2\}$ stands for the upper boundary value of the reference data of the adjacent $C - 2$ observation nodes.

(5) Based on the described extreme value detection coefficient α_1 , the temporal consistency detection coefficient α_2 and the spatial consistency detection coefficient α_3 of the data, the coefficient of evaluation of data authenticity θ is calculated by using formula (5):

$$\theta = \begin{cases} \frac{w_1\alpha_1 + w_2\alpha_2 + w_3\alpha_3}{w_1 + w_2 + w_3}, & if \ \ \alpha_1 \geq 0, \ \ \alpha_2 \geq 0 \\ -\frac{w_1\alpha_1 + w_2\alpha_2 + w_3\alpha_3}{w_1 + w_2 + w_3}, & otherwise \end{cases} \tag{5}$$

wherein w stands for the weight of the corresponding detection coefficient.

(6) In evaluating the described coefficient of evaluation of data authenticity θ, use the interval threshold to evaluate the authenticity of the data authenticity coefficient. When $\theta \in (0, 0.5]$, the current data are believed to be reliable; otherwise, the data are believed to be unreliable.

2.2.2. Training module

The main function of the training module is to establish a regression model between the sensor data and the real data so as to provide model parameters for the next step of calibrating the data using the correction module. The reason for building this module is that relatively low cost sensors are used in urban unit observation to achieve the goal of deploying a large number of such instruments in an urban unit. In order to make the data collected by these low-cost sensors reliable, we need to calibrate the data by using the existing data collected by sensors with high accuracy, i.e., the sensors of professional automatic weather stations. In this study, we used a method based on the Supporting Vector Machine (SVM) (Suykens and Vandewalle, 1999) to set up the training module, which can establish regression models according to the time series of a certain observation point and the time series of the adjacent higher precision observation points. The input vector is mapped to a high-dimensional eigenvector space, and the optimal regression function is constructed in the high-dimensional eigenvector space to solve the nonlinear regression problem, including the following steps:

(1) Obtain the observed data of a meteorological element at the current observation location within $M \times T$ hours

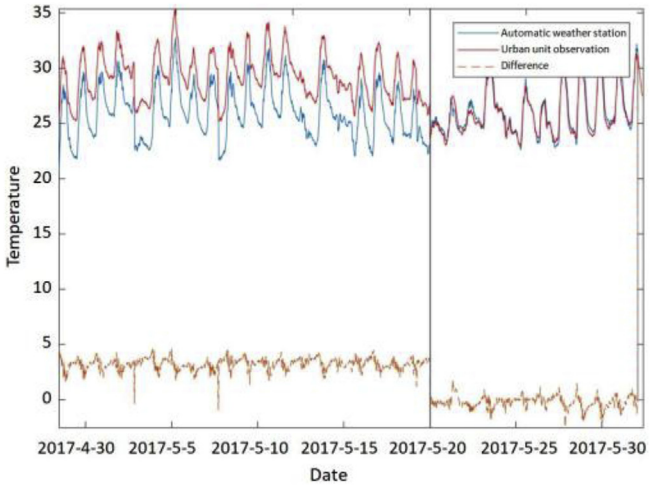

Fig. 2. The comparison between the air temperature data from urban unit observation and those from the automatic weather station observation.

$X_{MH} = \{x_i | i = 1,2,...,M \times T \times S\} \in \mathbb{R}^{(M\times T\times S)\times 1}$ and the input observed data of the corresponding meteorological element in the adjacent C observation nodes in terms of spatial geographic location within $M \times T$ hours $X_{MR}^k = \{x_i^k | i = 1,2,...,M \times T \times S\} \in \mathbb{R}^{(M\times T\times S)\times 1}$, wherein $k = 1,2, ...,C$;

(2) Use a sliding window with a sequence length of $T \times S$ and a step length of L to perform the sequence selection operation on X_{MH} to obtain the input $\hat{X}_i \in \mathbb{R}^{(T\times S)\times 1}$, wherein $i = 1,2, ...,N$, of the N group training samples for the current observation node, and use the next observed value of the current sliding window as the output of the training samples $Y = \{y_i | i = 1,2,...,N\} \in \mathbb{R}^{1\times N}$;

(3) Use a sliding window with a sequence length of $T \times S$ and a step length of L to perform the sequence selection operation on X_{MR}^k to obtain the input $\hat{X}_{i,k} \in \mathbb{R}^{(T\times S)\times 1}$, wherein $i = 1,2, ...,N$; $k = 1,2, ...,C$, of the $N \times C$ group training samples for the adjacent C observation nodes;

(4) Perform canonical correlation analysis on the input sample of the kth adjacent observation node $\hat{X}_k \in \mathbb{R}^{(T\times S)\times N}$ and the input sample of the current observation node $\hat{X} \in \mathbb{R}^{(T\times S)\times N}$ to solve the projection matrix, so that the correlation coefficient ρ_k of $U_k = A_k^T \hat{X}_k$ and $V_k = B_k^T \hat{X}$ is maximum to yield the optimization function shown by formula (6)

$$\text{argmax}\,\rho_k = \frac{A_k^T \sum_{\hat{X}_k\hat{X}} B_k}{\sqrt{A_k^T \sum_{\hat{X}_k\hat{X}_k} A_k} \quad \sqrt{B_k^T \sum_{\hat{X}\hat{X}} B_k}} \tag{6}$$

wherein $\sum_{\hat{X}_k\hat{X}_k}$, $\sum_{\hat{X}\hat{X}}$ stand for the covariance matrixes of the input samples $\hat{X}_k$, $\hat{X}$ respectively, and $\sum_{\hat{X}_k\hat{X}}$ stands for the cross-covariance matrix of the input sample $\hat{X}_k$, $\hat{X}$;

(5) Use the Lagrange multiplier to solve the described optimized function to yield the projection matrix $A_k, B_k \in \mathbb{R}^{(T\times S)\times P}$ and the post-projection input sample matrix $U_k, V_k \in \mathbb{R}^{P\times N}$, wherein P stands for the dimension projected into the subspace;

(6) Splice C pairs of sample matrixes U_k, V_k to obtain the characteristic matrix of N groups of training samples $H = [U_1^T, V_1^T, U_2^T, V_2^T, ..., U_C^T, V_C^T]^T$;

(7) For the characteristic matrix $H = \{h_i | i = 1,2,...,N\} \in \mathbb{R}^{(P\times C\times 2)\times N}$, and the output of the training samples $Y = \{y_i | i = 1,2,...,N\} \in \mathbb{R}^{1\times N}$, suppose there is a linear regression function $f(h_i) = w\ h_i + b$, where the difference between y_i and $f(h_i)$ is very small, then $f(h_i)$ can be used to predict the y_i value of an arbitrarily inputted h_i;

(8) Use a support vector regression machine to establish a regression prediction model, and the optimization function of the support vector regression machine is as follows:

$$\min \frac{1}{2}\|w\|^2 + \eta \sum_{i=1}^{N} \xi_i + \xi_i^*$$
$$s.t. \begin{cases} y_i - w\ h_i - b \le \varepsilon + \xi_i \\ w\ h_i + b - y_i \le \varepsilon + \xi_i^* \\ \xi_i \ge 0,\ \xi_i^* \ge 0 \end{cases} \tag{7}$$

wherein ε stands for the maximum prediction error, ξ_i, ξ_i^* stand for the relaxation factors, which are used to process the sample data points with the prediction errors exceeding ε; η stands for the penalty factor, which is used to restrict the sample data points with prediction errors exceeding ε;

The optimization function of the support vector regression machine is solved by Lagrange duality method to obtain w and b.

2.2.3. Correction module

After the initial quality control through the judgment module, the observed data can be further calibrated by the regression model established by the training module of the data processor. The specific steps are as follows:

(1) Obtain $T \times S$ historical input data of the current observation node and adjacent C observation nodes within T hours at the current time $X_H = \{x_i | i = 1,2,...,T \times S\} \in \mathbb{R}^{(T\times S)\times 1}$ and $X_{HR}^k = \{x_i^k | i = 1,2,...,T \times S\} \in \mathbb{R}^{(T\times S)\times 1}$, respectively, wherein $k = 1,2, ...,C$, and then obtain the projection matrixes A_k, B_k for subspace projection through the aforementioned optimization function:

$$u^k = A_k^T X^k$$
$$v^k = B_k^T X \tag{8}$$

(2) Splice vectors u^k, v^k gone through C group projection to obtain the feature vector of the sample to be predicted, shown as below:

$$h = [u_1, v_1, u_2, v_2, ..., u_C, v_C] \tag{9}$$

(3) Input the feature vector h into the regression function $f(h)$ to yield the predicted value of the input sample $y' = f(h)$; then output the predicted value as the corrected value of abnormal data.

Fig. 2 shows the comparison of the air temperature between the urban unit observation instrument and the professional automatic weather station at the same location in an outdoor environment in Shenzhen. We placed the urban unit observation instruments into a thermometer shelter to collect data for performing the comparison. During the period from April 30 to May 20 of 2017 the data from the urban unit observation instrument were not calibrated, and the average value of the absolute error reached as high as 0.62 °C. On the other hand, during the period from May 20 and 31, the calibration was performed, and the average value of the absolute error diminished to 0.17 °C, indicating that the accuracy of the urban unit microclimate measurement can be significantly improved solely by implementing the software with appropriate algorithms and without an increase in the cost of the hardware. The cost of the equipment utilizing the above algorithms is only 1/10 of that of the professional automatic weather station with similar function.

3. Application examples

3.1. The layout of the observation network

The minimum number of the sensors in an urban unit depends on the particular condition of the urban unit, such as the scale, the number of buildings or rooms. The target of the observation is also important to determine the minimum number of sensors. For general application, one sensor for each room of the urban unit are recommended to ensure

Fig. 3. The map of the campus.

to collect “enough” information. In this study, taking a school campus in Shenzhen as an example, the aforementioned technology on urban unit microclimate observation is tested. Fig. 3 is a map of the campus. There are a total of 4 buildings on the campus. All the buildings are 5-floor buildings oriented from northeast to southwest, and are respectively labeled as A, B, C, and D from south to north. A total of 25 urban unit microclimate observation instruments have been deployed throughout the campus, ranging from the basement floor to the fifth floor. Though the instruments are not installed in all rooms of the campus, they are deployed as many as possible in the areas with frequent student activities, such as student classrooms and other functional rooms. After a thorough calibration test, the observation system was put into operation in September 2017, and all the instruments were set up to collect data once every minute.

3.2. Monitoring data products

Fig. 4 shows the 3D rendered cloud map of the observed data at 22:00 p.m. on Sunday, May 13, 2018. It is not difficult to see from Fig. 4a that the indoor air temperature on the campus was still relatively high even after sunset, with the air temperatures of most rooms being in the range of being “warm to hot”, and the air temperatures of some rooms reaching the level of being “extremely hot”. This was mainly due to the fact that on the Sunday night no student was attending class on the campus, so the air conditioners were turned off. Therefore, the monitoring data reflected the typical indoor air temperature in the early summer season in the subtropical climate zone. It can also be seen that in the low floors of the middle section of Building B, the temperature was in the state of being suitable. Actually, these rooms are the teachers' offices, where the air conditioners had been working in order to keep the indoor air temperature within a comfortable range because there were teachers working overtime to prepare lessons. Fig. 4b is a graphical product of relative humidity. It can be seen in the figure that most areas were in the state of being “moderately humid to humid”, indicating that the indoor relative humidity was high without artificial intervention. Considering both the air temperature and the relative humidity, it can be found that if there is no artificial intervention such as air conditioning, the indoor environment is quite muggy even in the night in the early summer of the subtropical climate zone, and the comfort level is generally poor, which is consistent with some previous conclusions from outdoor meteorological observations–due to the effects of urbanization and global change, it has also become to be hot and uncomfortable at night in Shenzhen (Li et al., 2015).

The managers on the campus can quickly decide to perform appropriate activities in the target rooms of the unit to regulate the microclimate of the rooms in the light of the graphic products similar to those shown in Fig. 4. If someone wants to achieve the automated control of the unit's indoor microclimatic environment, he or she can directly link the switches and gears of the air conditioners or humidifiers with the observed data of indoor air temperature and relative humidity, by setting to trigger the switches or gears of these regulators when a certain threshold value is reached, to achieve self-regulation of the indoor microclimate environment.

3.3. Comparison and analysis of monitored data

The intensive monitored data of urban units can help to understand the differences between the indoor microclimate and the outdoor microclimate. In this study, a hot period from September 11 to 15 of 2017 when the students were on the campus, and a cold period from February 1 to 5 of 2018 when the students were on vacation, were selected for data analysis. The data from 4 representative monitoring points at different floors of different buildings in different function rooms on the campus and an automatic weather station near the campus (with a distance of approximately 2.6 km) were selected for the comparative analysis. It should be noted that the first floor of Building A is the library, the second floor of Building B and Building C are the classrooms, the fifth floor of Building B is the laboratory. The indoor air conditioning was not turned on during the period when the data were collected for comparison, so that the difference between indoor and outdoor air temperatures without artificial intervention could be compared and analyzed. Though the doors and windows were generally closed during the observation period, they were occasionally open when there are students in class. The windows and doors are closed in the evening and during the vacation. In order to obtain as smooth data as possible, the hourly average values of the observed data are

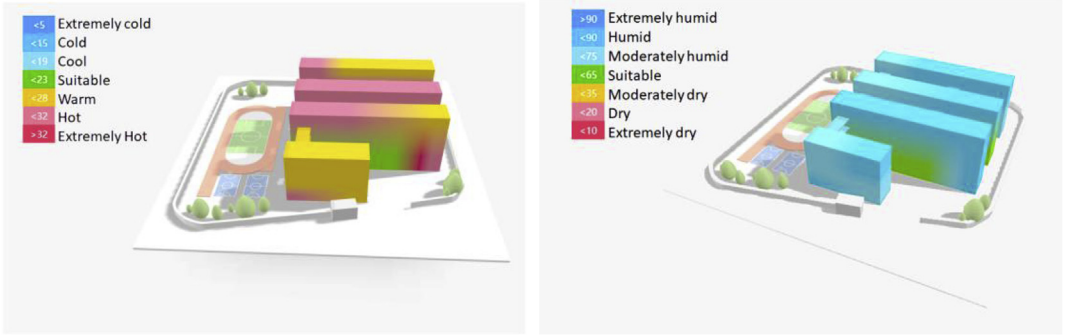

(a) (b)

Fig. 4. The examples of the indoor microclimate monitoring products on the campus (a. air temperature, b. relative humidity).

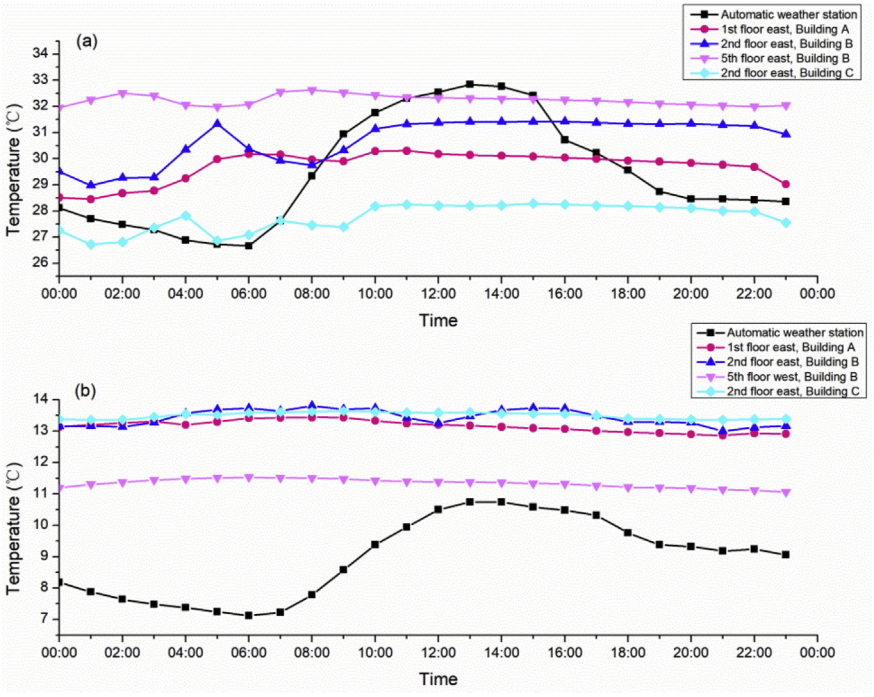

Fig. 5. The daily air temperature variations during the hot period (a) and the cold period (b).

calculated at each fixed time point of the 5 days during the hot and the cold periods, and the daily cycle variation data of the two periods (hot and cold) are obtained (Fig. 5).

The analysis shows that the air temperature of the automatic weather station exhibited a significant diurnal variation, which reached the lowest value before sunrise, and reached the highest value in the afternoon. However, there was almost no obvious diurnal variation in the indoor air temperature within the urban unit, which indicates that the indoor microclimate is obviously affected by the building envelop (Künzel et al., 2005; Liu et al., 2008; Mirrahimi et al., 2016). In addition, the air temperatures at the 4 monitoring points are different from each other, though all these points are all in indoor environment. Furthermore, the differences of the average temperatures among the different monitoring points were quite large, especially during the hot period (Fig. 5a). The air temperature ranges of the 4 monitoring points were all between the daily maximum and minimum temperatures of the automatic weather station in the open space. The daily temperature differences between the indoor monitoring points and the automatic weather station were between −1.7 ℃ and 2.8 ℃.

During the cold period (Fig. 5b), the air temperature variation tendencies exhibited different characteristics from those during the hot period. The air temperature of each of the 4 indoor monitoring points at each time point was higher than the average daily maximum value of the automatic weather station. The air temperature of the monitoring point on the west side of the fifth floor of Building B was the lowest among those of the 4 monitoring points. It was also the point with air temperature being relatively close to the outdoor one. Through an on-site inquiry, it is learned that the doors and windows were not closed during the observation period, causing the monitoring point colder than others. The temperatures of the other 3 points were close to each other. We can see that air convection significantly affect the indoor temperature. As can be seen from the figure, the difference between indoor and outdoor temperatures reached maximum values before sunrise and slowly diminished after sunrise. Generally speaking, the mean daily indoor air temperature was nearly 4.5 ℃ higher than the mean daily outdoor air temperature except the fifth floor of Building B.

The analysis of the relative humidity data shows that the data from automatic weather station had obvious diurnal variation. Generally speaking, the relative humidity was high during night, then diminished gradually after sunrise, and reached the lowest value around noon. The primary reasons why the relative humidity during the night is higher than that during the daytime are that the solar radiation is weaker, the air temperature is lower and boundary layer height is lower during night, which leads to the water vapor to be easily suppressed in the surface layer. However, the indoor observed data showed different trends from those in outdoor environment. Firstly, the variation range of the indoor relative humidity was generally smaller than that of the outdoor relative humidity. Secondly, the hot period and the cold period exhibited different variation tendencies. During the hot period (Fig. 6a), the relative humidity was at low levels from 23:00 to just prior to sunrise on each day, gradually increased after sunrise, and gradually stabilized before decreased after 22:00 in the night. Whereas during the cold period, the variation range of the indoor relative humidity was much narrower, and the variations in different rooms were quite different. The reasons why there are differences of the indoor relative humidity during the two periods are related to the working schedule of the school. During the hot period, the students and teachers were attending classes in rooms. The water vapor released by respiration of crowded people may be the major reason leading to rise of the indoor relative humidity after 8:00 on each day. This indicates that although the human beings have little influence on the relative humidity in open space, it may significantly affect the relative humidity in indoor space. The cold period was just within a holiday period, when people were not working in every room. Therefore, different rooms showed different characteristics of the relative humidity variation. Due to open the doors and windows, relative humidity is also closer to the outdoor one.

4. Conclusions

In this study, the concept of microclimate observation within urban unit is proposed, and an observation experiment on a campus in Shenzhen, China is carried out. The conclusions are as follows:

(1) The data quality control and calibration software based on appropriate algorithms can significantly reduce the cost of single microclimate observation instrument without compromising the accuracy

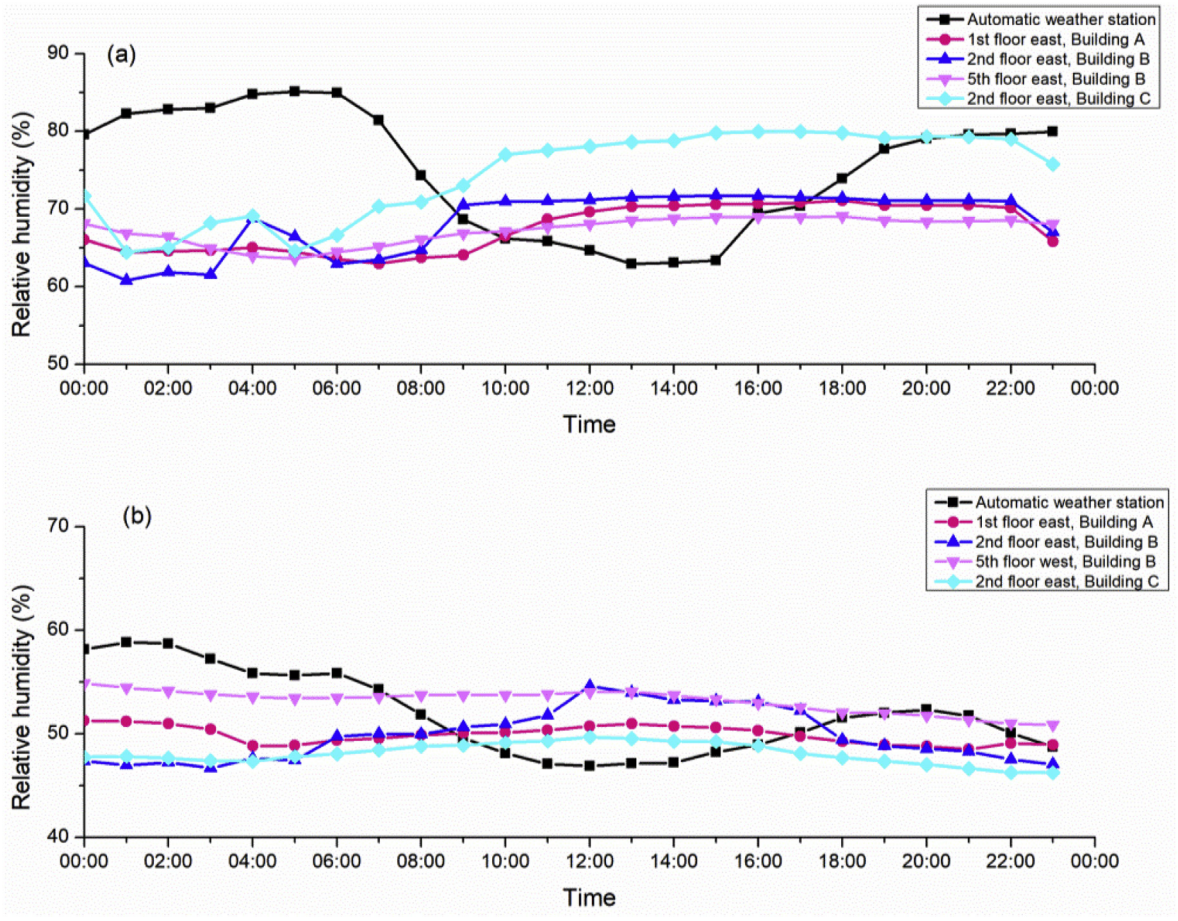

Fig. 6. The daily relative humidity variations during the hot period (a) and the cold period (b).

of the observed data. In the current study, an instrument capable of measuring 9 elements, namely, air temperature, humidity, ultraviolet, $PM_{2.5}$, formaldehyde, light, TVOC, noise and CO_2, is produced by using the precision integration technology. Consequently, its size is smaller than that of a traditional meteorological observation system and its cost is only 1/10 of that of a professional automatic weather station, which makes it suitable for being densely deployed within the urban units.

(2) The urban unit microclimate observation network established based on the Internet of things technology can precisely describe the heterogeneity of the microclimate environment in the urban units. It can provide the support for taking appropriate measures to adjust the microclimate environment for people's more comfortable working, living and studying in the urban units. At the same time, the microclimate data with high spatial and temporal resolution and high precision within the urban units can also provide the external parameters for the automatic control of the intelligent environment conditioners in the urban units.

(3) The analysis of the air temperature data shows that there is no significant diurnal variation for air temperature observed in the indoor environment, which is quite different from the observed data from the outdoor automatic weather station. The daily average air temperatures observed in the indoor environment are also quite different from those observed by the outdoor stations, indicating that the meteorological observation in open space does not have much reference value to the indoor environment of the urban units. At the same time, the observed data at different indoor monitoring points are quite different from each other. The observed data at the indoor monitoring points are closely related to the specific environment where they are in.

(4) The analysis on the relative humidity data shows that the variation rules of the indoor relative humidity are quite different from those in open space. Both the people in the room and the surrounded environment may affect the indoor relative humidity, further indicating the complexity and high heterogeneity of the indoor microclimate.

It can be expected that as the microclimate observation method proposed in this study could be gradually applied in more urban units, and the microclimate data could be acquired in a broader range. These big data can be expected to play an important role in the quality management and adjustment of the urban climatic environment, power dispatching, building energy efficiency and urban design.

Acknowledgements

This project is supported by the National Key Research and Development Plan of China (Grant No. 2016YFC0203600).

Appendix A. Supplementary data

Supplementary data related to this article can be found at https://doi.org/10.1016/j.pce.2018.08.003.

References

Evans, D., Conrad, C.L., Paul, F.M., 2003. Handbook of Automated Data Quality Control Checks and Procedures of the National Data Buoy Center. NDBC Technical Document 03-02.

Fountain, M., Brager, G., de Dear, R., 1996. Expectations of indoor climate control. Energy Build. 24 (3), 179–182.

Grimmond, S., 2007. Urbanization and global environmental change: local effects of urban warming. Geogr. J. 173, 83–88.
Hilliaho, K., Nordquist, B., Wallentèn, P., Hamid, A.A., Lahdensivu, J., 2016. Energy saving and indoor climate effects of an added glazed facade to a brick wall building: case study. J. Build Eng. 7, 246–262.
Kalnay, E., Cai, M., 2003. Impact of urbanization and land-use change on climate. Nature 423, 528–531.
Künzel, H.M., Holm, A., Zirkelbach, D., Karagiozis, A.N., 2005. Simulation of indoor temperature and humidity conditions including hygrothermal interactions with the building envelope. Sol. Energy 78 (4), 554–561.
Li, L., Chan, P.W., Wang, D.L., Tan, M.Y., 2015. Rapid urbanization effect on local climate: intercomparison of climate trends in Shenzhen and Hong Kong, 1968-2013. Clim. Res. 63 (2), 145–155.
Liu, Y., Lam, J.C., Tsang, C.L., 2008. Energy performance of building envelopes in different climate zones in China. Appl. Energy 85 (9), 800–817.
McCarthy, M.P., Best, M.J., Betts, R.A., 2010. Climate change in cities due to global warming and urban effects. Geophys. Res. Lett. 37 (9), 232–256.
Mirrahimi, S., Mohamed, M.F., Haw, L.C., Ibrahim, N.L.N., Yusoff, W.F.M., Aflaki, A., 2016. The effect of building envelope on the thermal comfort and energy saving for high-rise buildings in hot–humid climate. Renew. Sustain. Energy Rev. 53, 1508–1519.
Morgan, C., de Dear, R., 2003. Weather, clothing and thermal adaptation to indoor climate. Clim. Res. 24, 267–284.
Oke, T.R., 1981. Canyon geometry and the nocturnal urban heat island: comparison of scale model and field observations. Int. J. Climatol. 1, 237–254.
Oke, T.R., 1997. Urban environments. In: Bailey, W.G., Oke, T.R., Rouse, W.R. (Eds.), The Surface Climates of Canada. McGill/Queens University Press, Montreal, pp. 303–327.
Silva, L.T., Carrilho, J.D., Gaspar, A.R., Costa, J.J., 2016. Indoor climate assessment: a case study at a business incubation centre. Sustain. Cities Soc. 26, 466–475.
Suykens, J.A.K., Vandewalle, J., 1999. Least squares support vector machine classifiers. Neural Process. Lett. 9, 293–300.
WMO, 2017. Guide to Meteorological Instruments and Methods of Observation. pp. 6 WMO-No.8.
Wolfson, N., Erez, J., Alperson, Z., 1978. Automatic real-time quality control of surface synoptic observations. J. Appl. Meteorol. 17, 449–457.